Available online at www.sciencedirect.com
ScienceDirect
Journal of Photochemistry and Photobiology A: Chemistry 191 (2007) 66–73
Journal of Photochemistry and Photobiology A:Chemistry
www.elsevier.com/locate/jphotochem

Fabrication of ZnO nanoparticles by pulsed laser ablation in aqueous media and pH-dependent particle size: An approach to study the mechanism of enhanced green photoluminescence

Chun He, Takeshi Sasaki *, Hiroyuki Usui, Yoshiki Shimizu, Naoto Koshizaki *

Nanoarchitectonics Research Center (NARC), National Institute of Advanced Industrial Science and Technology (AIST), Central 5, 1-1-1 Higashi, Tsukuba, Ibaraki 305-8565, Japan

Received 26 November 2006; received in revised form 12 March 2007; accepted 5 April 2007
Available online 8 April 2007

Abstract

ZnO nanoparticles have been fabricated by pulsed laser ablation (PLA) of a zinc target in surfactant-free aqueous solutions, and surface chemistry effects on the green photoluminescence of ZnO nanoparticles were also investigated. The conspicuously stable, well-defined ZnO nanoparticles with very narrow size distribution were obtained by ablation of the Zn target under surfactant-free acidic or basic conditions due to the increased surface charge of nanoparticles compared to those prepared in deionized water. However, the ZnO nanoparticles produced in NaCl solution strongly coalesced due to the decreased surface charge of nanoparticles. Moreover, the green-to-exciton emission intensity ratio progressively increased with the particle average size decrease. This suggests that larger surface area for smaller nanoparticles produced more oxygen defects in the ZnO nanoparticles. Further experimental results on passivation of the nanoparticles with a surfactant, lauryl dimethylaminoacetic acid betaine (LDA), and post-reduction of the surface charge of the ZnO suspension, indicated that the green emission from ZnO nanoparticles obtained under the acidic condition originated partially from surface oxygen defects, while the green emission from those under the basic condition is primarily due to the defects below the crystalline ZnO nanoparticle surface, not from the surface itself.

Keywords: ZnO nanoparticles; Green photoluminescence; Pulsed laser ablation (PLA); Aqueous media

1. Introduction

ZnO has received much attention as an effective luminescent material due to its relatively high efficiency as a novel, low-voltage phosphor and for its potential application in the green range for vacuum fluorescent and field emission displays [1–3]. Inspired by the application of ZnO, a few groups have started to investigate the nature of the green luminescence from ZnO [3–10]. Recent results proved that the ionized oxygen vacancy was the main defect for the recombination centers involved in the green luminescence of ZnO resulting from the recombination of a photogenerated hole with the ionized charge state of the defect [1,2,4,7,9], although other researchers hypothesized that extrinsic Cu impurities in the earlier study [11] and Zn vacancy [3,12] were the centers responsible for green luminescence. Despite the progress in studies on the green luminescence of ZnO, there are still unresolved issues as to what are the relevant native defects of this oxide, since most of the properties of ZnO depend in various ways on the defects that are present in the material [3].

A large variation of the green luminescence properties of ZnO, including the peak position by the preparation conditions, have already been reported in the literature, and these were generally related to morphology, structure, particle size, composition and crystallinity [1,4–7,9,10,13–18]. Until now, most of the well-defined ZnO crystals have been synthesized by a traditional method based on the high-temperature solid-state method [14,19–21] or the chemical-solution route [10,13,22,23]. These methods usually involve a post-annealing treatment process for crystallization of ZnO in a reducing or oxidizing atmosphere. Thus, the number of vacancies can be varied, leading to a change in the visible photoluminescence intensity. Furthermore, the

* Corresponding authors. Tel.: +81 29 8616333; fax: +81 29 8616355.
E-mail addresses: takeshi.sasaki@aist.go.jp (T. Sasaki), koshizaki.naoto@aist.go.jp (N. Koshizaki).

1010-6030/$ – see front matter © 2007 Elsevier B.V. All rights reserved.
doi:10.1016/j.jphotochem.2007.04.006

green emission arising from the oxygen vacancies is sensitive to the molecular species present at the surface [24,25]. Thus, it is difficult to prepare ZnO particles without any surface contamination by residual ions or chemical agents. In this regard, a fabrication method for crystalline ZnO with a native surface at room temperature is needed. Recently, pulsed laser ablation (PLA) in liquid media has been found to provide an efficient route to prepare many kinds of nano-scaled materials [26–32]. The most important advantage of PLA in aqueous media is the ability to directly produce crystalline nanoparticles with a native surface, which cannot be achieved by other fabrication methods such as solid-state or chemical methods. In this PLA process in liquid media, strong reactions may take place between the ablated species and encountered solution molecules, and thus the nanocrystals can be prepared after rapid reactive quenching in liquid. However, the nanoparticles prepared by PLA in deionized water have a rather large size distribution because of the post-ablation coalescence of nanoclusters. Therefore, the growth control of nanoparticles and the stability of the dispersed ZnO nanoparticles are significantly important. One approach is to limit excess coalescence of nanoparticles by physical or chemical interaction with specific molecules such as surfactants [27–31]. In a previous study, stable ZnO nanocrystals with small size distribution were obtained by PLA in a surfactant aqueous solution above the critical micelle concentration (CMC). The green emission of the ZnO nanocrystals was partially or completely suppressed, since the micelle structure formation played a role in effectively passivating the oxygen vacancy. The surface of the nanoparticles, however, was no longer naked [31]. This makes it difficult to derive some conclusions on the origin of the green luminescence intensity and defect concentration related to surface and/or sub-surface defect in ZnO particles. This situation inspired us to prepare the small particles by controlling surface charge of nanoparticles via the pH value of the solution to inhibit their coalescence during PLA process.

In this study, small ZnO nanoparticles with native surfaces were prepared by pulsed laser ablation at room temperature in surfactant-free aqueous media. It was expected that ZnO nanoparticles with green emission can be obtained by PLA in surfactant-free aqueous media since high density surface defects are possibly formed by rapid quenching process of PLA in liquid inducing charged particle surface. One further aim was to examine the enhancement mechanism of green photoluminescence of ZnO nanoparticles and the oxygen vacancies from the surface and/or the sub-surface of the nanoparticles contributed to the green emission for ZnO nanoparticles.

2. Experimental

ZnO nanoparticles were produced by pulsed laser ablation of a Zn plate (99.99%) placed on the bottom of an open Pyrex vessel filled with 10 mL of deionized water (>18 MΩ, pH 7.51) or various aqueous solutions. The aqueous solutions of HCl (pH 5.36) and NaOH (pH 11.98) were prepared from standard solutions of 0.1 M HCl and 0.1 M NaOH. A NaCl aqueous solution in 10 mM (pH 7.15) was obtained by dissolving reagent-grade NaCl. The surface of the Zn plate was polished with 600-grade emery paper before each experiment. A focused Nd:YAG laser (Spectra-Physics, LAB-150-10) operated at 10 Hz with a wavelength of 355 nm and pulse width of 7 ns was vertically irradiated onto a Zn plate placed in aqueous solution. The laser beam was focused on the target plate surface with a beam size of 1.0 mm in diameter using a quartz lens with a focal length of 250 nm. In general, laser intensity of 100 mJ/pulse was employed to ablate a zinc plate for 60 min. After ablation, all solutions became slightly turbid but were still transparent.

The optical properties of the obtained nascent suspensions were measured at room temperature by a Shimadzu UV-2100PC spectrophotometer and a Shimadzu RF-5300PC fluorescence spectrophotometer without a cutoff filter at room temperature under an excitation of wavelength 340 nm (3.65 eV) (340 nm was selected as excited wavelength to avoid the overlap of the exciton emission and solvent Raman peak, so that the solvent Raman peak can be subtracted from the PL spectrum during the calculation of the ratio of green emission intensity to exciton emission intensity). Zeta potential measurements were performed using a Zetasizer Nano-ZS meter. These colloid suspensions were centrifuged at 50,000 rpm for 45 min by an ultracentrifuge (Hitachi CS100GXL with an S100AT6 rotor) to purify and concentrate the products. Electron micrographs using a field emission scanning electron microscopy (FESEM, Hitachi S-4800) and a transmittance electron microscopy (TEM, JEOL JEM-2010) were obtained from nanoparticles by placing a drop of the suspension on a carbon-coated copper grid. Each size distribution of the nanoparticles was obtained by measuring the diameters of 100 nanoparticles on a given FESEM image. X-ray diffraction (XRD, Rigaku RAD-C) measurement using Cu Kα line ($\lambda = 0.15406$ nm) was performed for the dried film from the concentrated suspension on a quartz glass.

3. Results and discussion

3.1. Characterization of ZnO nanoparticles

Fig. 1 depicts X-ray diffraction patterns of nanoparticles obtained by PLA of a Zn plate in different aqueous solutions. For all fabrication conditions, XRD data show that these nanoparticles possessed the hexagonal wurtzite structure with lattice constants of $a = 3.247$ and $c = 5.202$ Å, which were consistent with the values in the database of ZnO (JCPDS 89-1397). No diffraction peak from Zn or other impurities was detected.

Fig. 2 presents the TEM images of ZnO nanoparticles produced in water and HCl solution (pH 5.36). They are spherical, and the electron diffraction patterns in the insets reveal that ZnO nanoparticles were formed by laser ablation of a Zn plate in these aqueous media. The nanoparticles produced in HCl (Fig. 2b) were comparatively small. Fig. 3 compares the size distribution of ZnO nanoparticles produced in different aqueous media. The average particle size and the standard deviation of particle size produced in HCl and NaOH solutions were smaller (15 ± 6 nm for HCl, pH 5.36; 20 ± 8 nm for NaOH, pH 11.98) than those prepared in deionized water (23 ± 11 nm, pH 7.51). In our previous study on ZnO nanoparticle preparation in various surfactant solutions, amphoteric surfactant LDA provided the smallest size

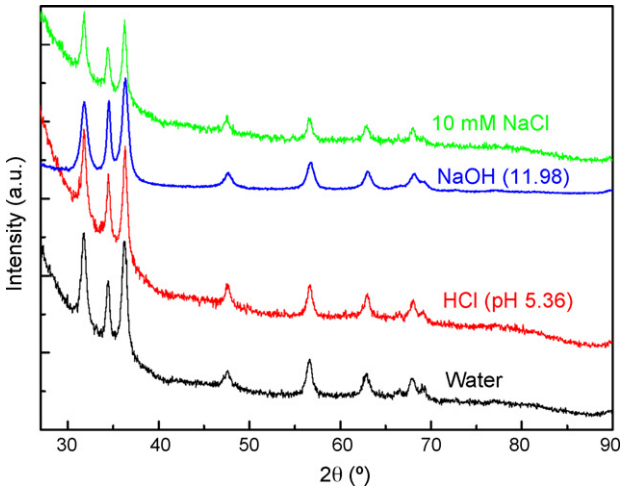

Fig. 1. XRD spectra of ZnO nanoparticles obtained by laser ablation in deionized water and aqueous solutions.

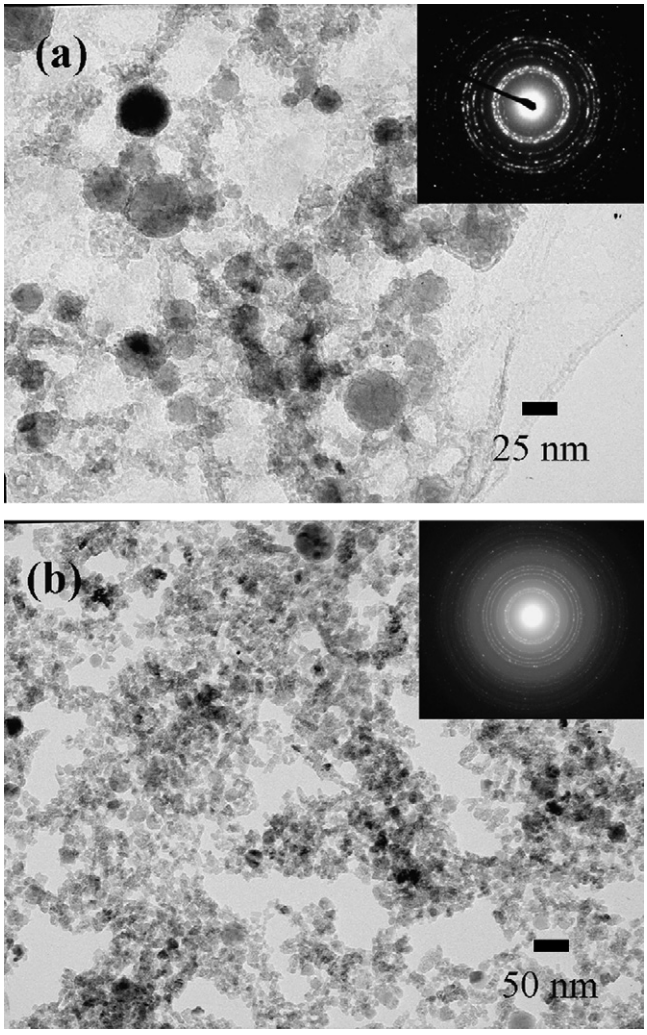

Fig. 2. TEM images of ZnO nanoparticles prepared by PLA of Zn in (a) deionized water (pH 7.51); (b) HCl solution (pH 5.36). Insets display the selected area electron diffraction pattern.

and standard deviation of produced ZnO nanoparticles [31]. However, the nanoparticles produced in surfactant-free HCl and NaOH solutions had comparable average size and standard deviation to those produced in LDA surfactant solution. These results indicate that the presence of acid or base controlled the nanoparticle growth during the PLA process in aqueous solution; i.e. the population of the large nanoparticle presented in deionized water under identical ablation conditions was suppressed under the acidic and basic media. However, the average particle size and the standard deviation of particle size produced in 10 mM NaCl solution was 26 ± 15 nm, larger than those prepared in water. Fig. 4 presents the absorption spectra of ZnO nanoparticles produced in different aqueous media. As can be seen, the absorption of ZnO produced in HCl and NaOH was much larger in UV range than that of nanoparticles produced in deionized water, which is attributed to enhanced Rayleigh scattering [33,34], due to the production of much smaller nanoparticles in HCl and NaOH. Furthermore, it was observed that ZnO nanoparticles prepared at pH 5.36 or pH 11.98 exhibited much conspicuous stability with no obvious change of the corresponding optical spectrum during aging for several days. In contrast, the absorption edge of ZnO produced in the NaCl solution was broader and weaker than that of nanoparticles produced in water, indicating the aggregation of nanoparticles or formation of larger nanoparticles.

3.2. Average particle size and photoluminescence of ZnO nanoparticles in different media

The typical photoluminescence spectra of ZnO produced in the different media are presented in Fig. 5. All the spectra exhibited an UV emission band around 3.40 eV (365 nm). The peak at 3.25 eV (382 nm) can be attributed to a solvent Raman peak at 0.40 eV (3240 cm^{-1}, corresponding to an OH-vibration) below the excitation energy of 3.65 eV (340 nm) [4,31,35]. The intense broad emission centered at 2.30 eV (540 nm) was also observed in the green region. There are two kinds of emission bands of UV and green in the ZnO crystals [1,2,4,6,7,9,10,13,25]. The emission in the UV region is attributed to the recombination between electrons in the conduction band and the holes in the valence band (exciton emission). The green emission is related to the defects in ZnO, and the peaks from 2.13 to 2.51 eV were attributed to oxygen vacancies [1,5–7,9,10,13,14,16–18]. In our present study, the green emission at 2.30 eV from ZnO originated from oxygen vacancies because nanoparticles prepared by PLA were grown under insufficient oxidation conditions [29,31]. The inhomogeneous broadening of the green band in all cases resulted from a distribution in nanoparticle sizes, according to some reports [25,35].

It should be noticed from Fig. 5 that the green emission intensity was strong compared to the exciton emission intensity when ZnO was produced in acidic or basic media, while the green emission intensity was somewhat weaker than the exciton emission intensity when ZnO was produced in salt solution or deionized water. Generally, these emission processes compete with each other, and this means that the green emission process must involve a step in which the photogenerated hole is efficiently trapped somewhere in the particles [35]. The rate of this

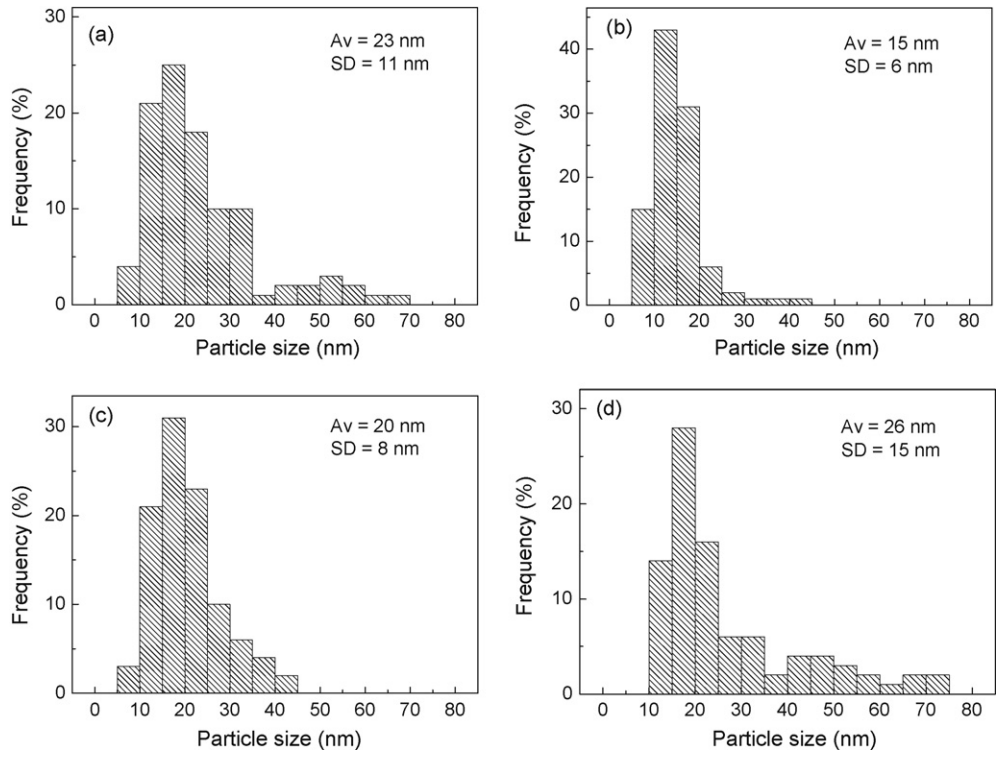

Fig. 3. Size distribution of ZnO nanoparticles prepared by PLA of Zn in (a) deionized water (pH 7.51); (b) HCl solution (pH 5.36); (c) NaOH solution (pH 11.98); and (d) 10 mM NaCl solution (pH 7.15). Av and SD present the average and standard derivation of the corresponding particle size distribution.

hole trapping must be much faster than the recombination of the exciton emission for the strong green emission of ZnO produced in acidic or basic media. Efficient and fast trapping of the photogenerated holes at the surface sites is expected due to the large surface-to-volume ratio of smaller nanoparticles produced in acidic or basic media.

The above results indicated that OH^- and H^+ interacted with the ZnO surface and controlled the growth of nanoparticles. They also affected the green emission. To clarify the effect of OH^- and H^+ concentration, we measured the pH dependence of zeta potential of ZnO nanoparticles produced by PLA of Zn in 10 mM NaCl aqueous solution with different pH values adjusted by adding diluted HCl or NaOH. A conductive NaCl aqueous solution was required for precise zeta potential measurement. As shown from curve a in Fig. 6, the zeta potential gradually decreased from a large positive value on the acidic side to a large negative value on the basic side, by crossing the zero value when the pH value was around 9.5. Above or below this crucial pH, the absolute value of zeta potential increased and nanoparticles were charged. This charging led to an increase of the electrostatic repulsion by exceeding the van der Waals attractive forces, and hence disturbed the coagulation.

The zeta potential measurement of ZnO nanoparticles as a function of pH confirmed the presence of hydroxyl groups

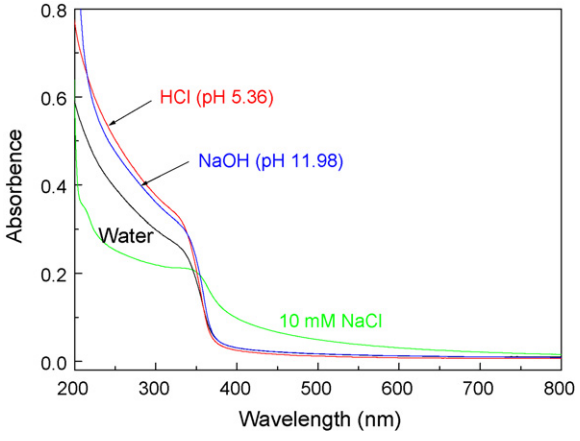

Fig. 4. Absorption spectra of ZnO nanoparticles prepared by PLA of Zn in deionized water and aqueous solutions.

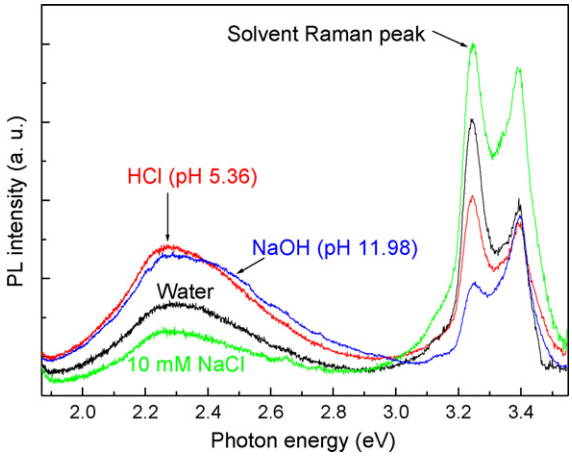

Fig. 5. Photoluminescence spectra of ZnO nanoparticles prepared by PLA of Zn in deionized water and aqueous solutions. Excitation wavelength: 340 nm (3.65 eV). Slit width: ±3.0 nm.

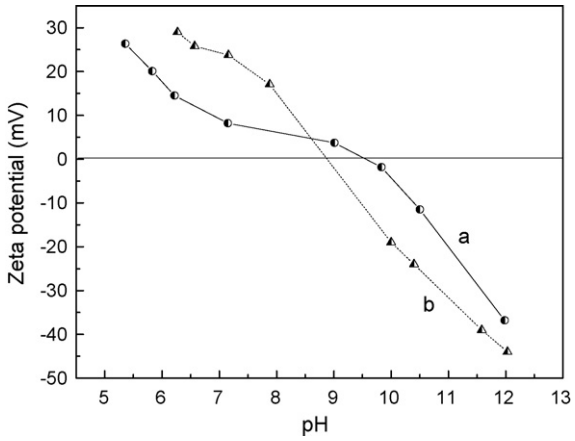

Fig. 6. Zeta potential of ZnO nanoparticles (a) produced by PLA of Zn in NaCl aqueous solution (10 mM) with different pH values adjusted by adding dilute HCl or NaOH, and (b) produced by PLA of Zn in deionized water and subsequent pH adjustment by HCl or NaOH.

on the ZnO nanoparticle surface. Indeed, the concentrations of these groups ($–ZnOH_2^+$, –ZnOH, $–ZnO^-$) depend on the pH of the solution [36]. The $–ZnOH_2^+$ and –ZnOH are dominant at lower pH, while $–ZnO^-$ is dominant at higher pH. The high absolute surface charge of the nanoparticles produced in HCl or NaOH solution provided repulsive force between nanoparticles and suppressed the growth through coagulation. The large ZnO nanoparticles produced in salt solution were also related to the low surface charge, as estimated from the zeta potential after laser ablation of 7 mV. This result indicates that chlorine ions from NaCl reacted with the $–ZnOH_2^+$, transferring their negative charge to the positive nanoparticles [32], so that the net surface charge of ZnO decreased. Therefore, the nanoparticles were grown in the PLA process in salt solution under reduced electrostatic repulsion between the nanoparticles.

To better understand the pH effect, we investigated the average size and the green-to-exciton emission intensity ratio of ZnO nanoparticles produced in HCl or NaOH solutions with various pH values. As can be seen from curve A in Fig. 7a, their photoluminescence properties strongly depended on the pH value. The green-to-exciton emission intensity ratio decreased as solution pH increased to 9.5 with the lowest green emission and then increased with further pH increase above 9.5. The strong green luminescence was achieved for ZnO nanoparticles produced in aqueous media above or below the crucial pH. It should be noted that the pH value 9.5 with a lowest green emission matched well with the pH value having zero zeta potential. Combined with the results that smaller nanoparticles were obtained in aqueous solution with relatively lower or higher pH (curve B in Fig. 7a), it is obvious that the enhanced green luminescence intensity is related to the size of ZnO nanoparticles. Indeed, according to previous studies, the green intensity is strongly dependent on defect concentration [2,6,10,37]. The results demonstrate that the green-to-exciton emission intensity ratio progressively increased as the particle size decreased. Since in the present experiment, ZnO nanoparticles were prepared by PLA in aqueous solutions under the same experimental con-

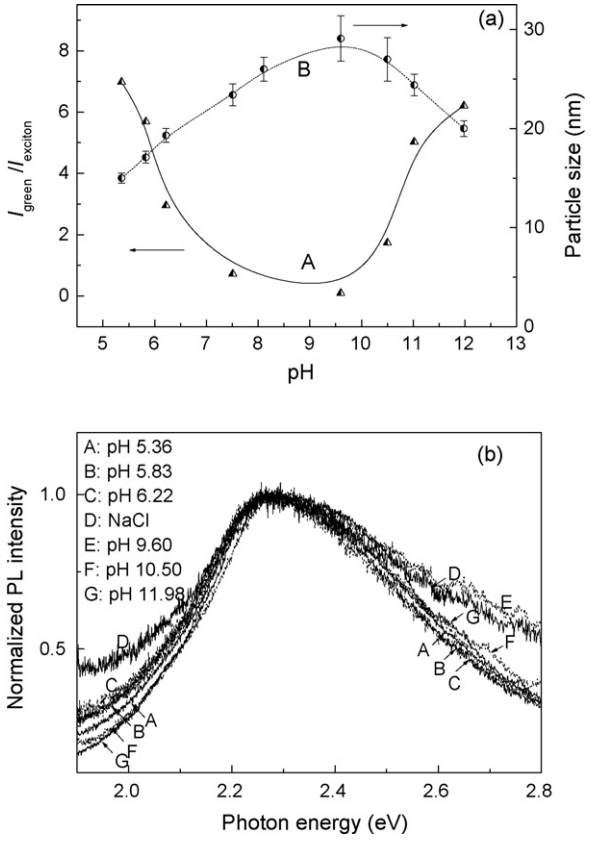

Fig. 7. (a) Integrated intensity ratio of green-to-exciton emission and average size of ZnO nanoparticles produced in solutions with various pH values. (b) Normalized curves of the green emission spectra of ZnO nanoparticles produced in solutions with various pH values. Excitation wavelength: 340 nm (3.65 eV). Slit width: ±3.0 nm.

ditions, except for the different pH value, it is possible that the density of oxygen vacancy on nanoparticles produced in different solutions is constant during each batch reaction. Therefore, it can be concluded that the higher surface area of smaller nanoparticles provides more defects in the ZnO nanoparticle surface region. In order to compare the variations of green emission peak shape at different pH values, the spectra were normalized to the maximum value (Fig. 7b). The main peak positions of green luminescence at 2.30 eV (540 nm) were not influenced by pH values and the narrower peak width of the green luminescence corresponded to the smaller nanoparticle. The progressive increase of the green emission with the same peak position at different pH values was not due to the appearance of a new kind of intrinsic defect in ZnO, but rather to the increase in the concentration of the same type of intrinsic defect. However, it is not clear from these data whether oxygen vacancies from the surface and/or the sub-surface of the nanoparticles contributed to the green emission for ZnO nanoparticles.

3.3. Post-treatment effects on emission intensity of ZnO nanoparticles

In an attempt to answer the remaining issues, the ZnO nanoparticles were fabricated for two typical conditions (pH

5.36 and pH 11.98) and the variation of the obtained photoluminescence spectra of ZnO was compared by adding 0.01 M of amphoteric surfactant, lauryl dimethylaminoacetic acid (LDA), to examine the effect of the post-quenching on green emission. Fig. 8a demonstrates that the visible emission was partially quenched and UV emission simultaneously increased by post-addition of LDA when ZnO was produced in an acidic condition. The zeta potential of the colloidal solution after addition of LDA was +22.0 mV, less than +30.0 mV of the nascent solution immediately after laser ablation. The decreased zeta potential indicates that the amphoteric LDA adsorbed electrostatically via the anionic carboxyl headgroup $–OOCCH_2(CH_3)_2N^+(CH_2)_{11}CH_3$ on the positively charged ZnO surface. Anionic oxygen in the surfactant molecules can occupy the oxygen vacancy sites on the ZnO nanoparticle surface, so that the oxygen vacancy can be complemented by coating the nanoparticles with LDA. This result indicates that part of the green emission originated from oxygen vacancies located on the surface, which were sensitive to surfactant molecules.

In contrast, Fig. 7b demonstrates that no significant change due to LDA addition was observed in the green emission intensity of negatively charged ZnO nanoparticles produced in the basic condition. Furthermore, the zeta potential was changed from −44.6 to −53.0 mV, a more negatively charged state, by LDA addition. This change is possibly explained as follows. The electrostatic interaction between negatively charged ZnO nanoparticles and anionic carboxyl groups at the end of LDA molecule is not dominant, leading to a weak interaction between ZnO and the nonpolar hydrophobic part of LDA, which probably directs the hydrophilic group outward to the polar water to form micelles due to hydrophobic interaction [38]. Thus, defects on the ZnO surface were not passivated at all, and the whole nanoparticle surface was more negatively charged due to the carbonyl group of LDA. Therefore, this data alone is not sufficient to determine whether the green emission from ZnO nanoparticles produced under the basic condition originated from defects on the surface or the sub-surface.

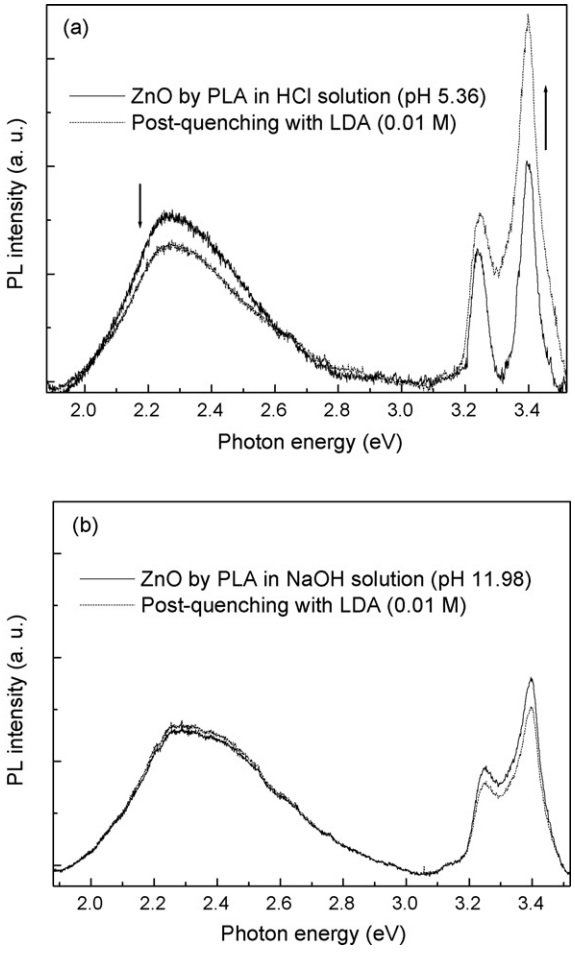

Fig. 8. Post-addition effect of LDA on the green emission of ZnO produced in (a) HCl solution (pH 5.36) and (b) NaOH solution (pH 11.98).

To further clarify whether green emission originates from the surface and/or the sub-surface of the ZnO nanoparticles produced under the basic condition, we compared the post-aggregation effects by pH change on the emission intensity under two typical pH conditions. First, we monitored the emission intensity change of the ZnO colloidal solution produced in the acidic condition at 5.36 by adding dilute NaOH solution to increase the pH value to 7.80, and then to 11.00 (from A to B and then to C in Fig. 9a). The intensity of the green emission decreased considerably while that of the exciton emission increased. Simultaneously, the absorbance decreased progressively with the addition of dilute NaOH solution to the ZnO colloidal solution, as depicted in the inset of Fig. 9a. Moreover, the zeta potential decreased when the pH was increased to 7.80 (curve b in Fig. 6), which induced the aggregation of nanoparticles. The results suggest that the decreased green emission might be associated with the decrease of oxygen vacancies on the surface and/or sub-surface of ZnO nanoparticles induced by nanoparticle aggregation. Although we cannot infer the exact fraction of defect concentration from surface or from sub-surface during this post-aggregation process that contributed to the decreased green emission, this post-aggregation may affect the defect concentration below the ZnO surface to some extent. However, the intensity of the green emission showed no obvious increase, as the pH value was re-adjusted to the acidic side at pH 6.5 again (from C to D in Fig. 9a), indicating that this post-aggregation process was irreversible and disaggregation did not proceed.

In contrast, the green emission intensity from ZnO nanoparticles produced in the NaOH solution (pH 11.98) exhibited only a slight change when the pH was decreased by adding dilute HCl solution to the ZnO colloidal solution (Fig. 9b). However, the decrease in absorption (the inset of Fig. 9b) and the absolute value of zeta potential (curve b in Fig. 6) indicates that small ZnO nanoparticles had experienced post-aggregation. The insignificant decrease of green emission is also related to the features of post-aggregation, which resulted in the decrease of defect concentration from the ZnO surface and/or the sub-surface. The fact that the zeta potential of ZnO nanoparticles produced under the basic condition was negative means that the oxygen vacancies on the ZnO surface can be passivated by the adsorption of hydroxyl ions in the solution. Therefore, the defect concentration of oxy-

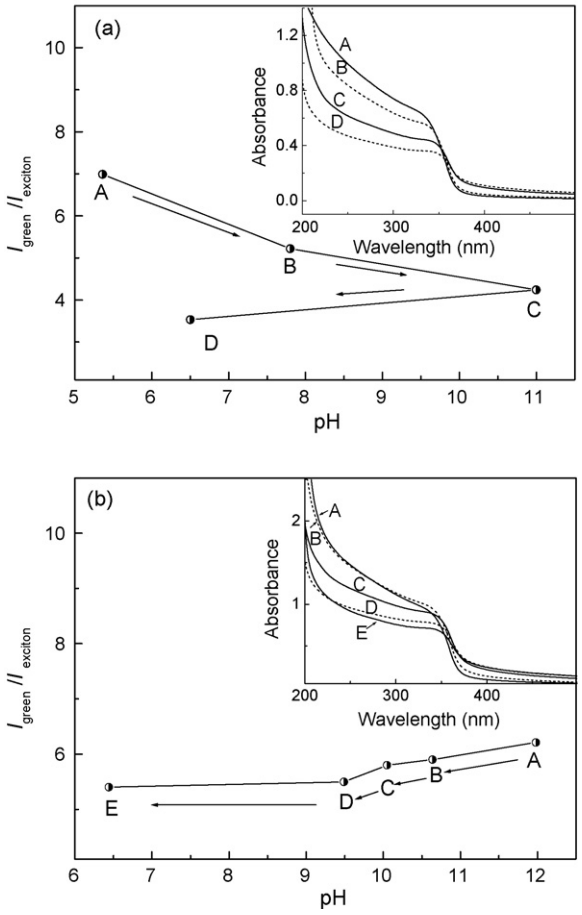

Fig. 9. Integrated intensity ratio of green-to-exciton emission from ZnO nanoparticles prepared by PLA of Zn in (a) HCl solution at pH 5.36, and their change by subsequent pH adjustment to 7.80, 11.00, and 6.50 using NaOH or HCl; and (b) NaOH solution at pH 11.98, and their change by subsequent pH adjustment to 10.64, 10.05, 9.49, and 6.44 using HCl. Excitation wavelength: 340 nm (3.65 eV). Slit width: ±3.0 nm. The inset displays corresponding adsorption spectra.

gen vacancy located at the nanoparticle surface is less than the former case, and the green emission centers are mostly attributed to oxygen vacancies from the sub-surface of nanoparticles, not from the surface.

4. Conclusion

Pulsed laser ablation of a zinc target in aqueous solutions was used to produce ZnO nanoparticles with particle size control. Very stable ZnO nanoparticles with very narrow size distribution were produced by ablation of a Zn target under acidic or basic condition due to the high absolute surface charge of nanoparticles. In contrast, the ZnO nanoparticles produced in NaCl solution coalesced strongly. Furthermore, the intensity of green emission increased while that of the exciton emission decreased as the particle size decrease due to more oxygen defects in the smaller ZnO nanoparticle. We found that the green emission from ZnO nanoparticles obtained under the acidic condition originated partially from surface defects, while the green emission from ZnO nanoparticles produced under the basic condition originated primarily from the defects below the crystalline ZnO nanoparticle surface, not from the surface itself.

Acknowledgements

Author CH wishes to express thanks to the Japan Society for the Promotion of Science (JSPS) for financial support for this work. This study was partially supported by the Industrial Technology Research Grant Program 2005 from the New Energy and Industrial Technology Development Organization (NEDO) of Japan.

References

[1] K. Vanheusden, W.L. Warren, C.H. Seager, D.R. Tallant, J.A. Voigt, B.E. Gnade, J. Appl. Phys. 79 (1996) 7983.
[2] C.M. Mo, Y.H. Li, Y.S. Liu, Y. Zhang, L.D. Zhang, J. Appl. Phys. 83 (1998) 4389.
[3] A.F. Kohan, G. Ceder, D. Morgan, C.G. Van de Walle, Phys. Rev. B 61 (2000) 15019.
[4] A. van Dijken, E.A. Meulenkamp, D. Vanmaekelbergh, A. Meijerink, J. Phys. Chem. B 104 (2000) 1715.
[5] S. Fujihara, Y. Ogawa, A. Kasai, Chem. Mater. 16 (2004) 2965.
[6] A.B. Djurisic, W.C.H. Choy, V.A.L. Roy, Y.H. Leung, C.Y. Kwong, K.W. Cheah, T.K.G. Rao, W.K. Chan, H.T. Lui, C. Surya, Adv. Funct. Mater. 14 (2004) 856.
[7] S.A. Studenikin, N. Golego, M. Cocivera, J. Appl. Phys. 84 (1998) 2287.
[8] N.Y. Garces, L. Wang, L. Bai, N.C. Giles, L.E. Halliburton, G. Cantwell, Appl. Phys. Lett. 81 (2002) 622.
[9] A. van Dijken, E.A. Meulenkamp, D. Vanmaekelbergh, A. Meijerink, J. Lumin. 87-89 (2000) 454.
[10] F.S. Wen, W.L. Li, J.H. Moon, J.H. Kim, Solid State Commun. 135 (2005) 34.
[11] R. Dingle, Phys. Rev. Lett. 23 (1969) 579.
[12] E.G. Bylander, J. Appl. Phys. 49 (1978) 1188.
[13] Z.Y. Xiao, Y.C. Liu, L. Dong, C.L. Shao, J.Y. Zhang, Y.M. Lu, D.Z. Zhen, X.W. Fan, J. Colloid Interface Sci. 282 (2005) 403.
[14] S.A.M. Lima, F.A. Sigoli, M. Jafelicci Jr., M.R. Davolos, Int. J. Inorg. Mater. 3 (2001) 749.
[15] J.Q. Hu, Y. Bando, J.H. Zhan, Y.B. Li, T. Sekiguchi, Appl. Phys. Lett. 83 (2003) 4414.
[16] J.Q. Hu, Y. Bando, Appl. Phys. Lett. 82 (2003) 1401.
[17] K. Vanheusden, C.H. Seager, W.L. Warren, D.R. Tallant, J.A. Voigt, Appl. Phys. Lett. 68 (1996) 403.
[18] Y. Dai, Y. Zhang, Q.K. Li, C.W. Nan, Chem. Phys. Lett. 83 (2002) 358.
[19] B.S. Li, Y.C. Liu, Z.Z. Zhi, D.Z. Shen, Y.M. Lu, J.Y. Zhang, X.G. Kong, X.W. Fan, Thin Solid Films 414 (2002) 170–174.
[20] Z.X. Fu, B.X. Lin, G.H. Liao, Z.Q. Wu, J. Cryst. Growth 193 (1998) 316.
[21] S. Ohara, T. Mousavand, M. Umetsu, S. Takami, T. Adschiri, Y. Kuroki, M. Takata, Solid State Ionics 172 (2004) 261–264.
[22] X.D. Gao, X.M. Li, W.D. Yu, J. Solid State Chem. 177 (2004) 3830.
[23] H.M. Xiong, D.P. Liu, Y.Y. Xia, J.S. Chen, Chem. Mater. 17 (2005) 3062.
[24] P.V. Kamat, B. Patrick, J. Phys. Chem. 96 (1992) 6829.
[25] C.L. Yang, J.N. Wang, W.K. Ge, L. Guo, S.H. Yang, D.Z. Shen, J. Appl. Phys. 90 (2001) 4489.
[26] C. He, T. Sasaki, Y. Zhou, Y. Shimizu, N. Koshizaki, Adv. Funct. Mater. (adfm.200700081) (In press).
[27] F. Mafuné, J. Kohno, Y. Takeda, T. Kondow, H. Sawabe, J. Phys. Chem. B 104 (2000) 8333.
[28] F. Mafuné, J. Kohno, Y. Takeda, T. Kondow, J. Phys. Chem. B 107 (2001) 4218.
[29] C.H. Liang, Y. Shimizu, T. Sasaki, N. Koshizaki, J. Phys. Chem. B 107 (2003) 9220.
[30] J.P. Sylvestre, A.V. Kabashin, E. Sacher, M. Meunier, J.H.T. Luong, J. Am. Chem. Soc. 126 (2004) 7176.

[31] H. Usui, Y. Shimizu, T. Sasaki, N. Koshizaki, J. Phys. Chem. B 109 (2005) 120.
[32] J.P. Sylvestre, S. Poulin, A.V. Kabashin, E. Sacher, M. Meunier, J.H.T. Luong, J. Phys. Chem. B 108 (2004) 16864.
[33] M.J. Eilon, T. Mokari, U. Banin, J. Phys. Chem. B 105 (2001) 12726.
[34] Y. Zhang, X. Wang, M. Ma, D.A. Fu, N. Gu, Z.H. Lu, J. Xu, L. Xu, K.J. Chen, J. Colloid Interface Sci. 266 (2003) 377.
[35] A. van Dijken, E.A. Meulenkamp, D. Vanmaekelbergh, A. Meijerink, J. Lumin. 90 (2000) 123.
[36] S.C. Liufu, H.N. Xiao, Y.P. Li, Powder Technol. 145 (2004) 20.
[37] J.J. Wu, S.C. Liu, Adv. Mater. 14 (2002) 215.
[38] Y. Ishikawa, Y. Shimizu, T. Sasaki, N. Koshizaki, J. Colloid Interface Sci. 300 (2006) 612.